

Mutant MEG3 Enhances the Activity of Telomerase by Increasing DNA Damage Repair in Human Liver Cancer Stem Cells

Shuting Song

Tongji University

Sijie Xie

Tongji University

Rushi Qin

Tongji University

Yanan Lu

Tongji University

Liyang Wang

Tongji University

Yingjie Chen

Tongji University

Xiaoxue Jiang

Tongji University

Dongdong Lu (✉ ludongdong@tongji.edu.cn)

Tongji University <https://orcid.org/0000-0002-7417-4172>

Research

Keywords: Mutant MEG3, H4K6Ac, Telomerase, DNA damage repair, Liver cancer stem cells

Posted Date: May 11th, 2021

DOI: <https://doi.org/10.21203/rs.3.rs-486093/v1>

License:   This work is licensed under a Creative Commons Attribution 4.0 International License.

[Read Full License](#)

Abstract

Background: Long noncoding RNAs have recently considered as central regulators in diverse biological processes and emerged as vital players controlling tumorigenesis. Although wild MEG3 acts as a suppressor in several cancers, the function of mutant MEG3 is also unclear during tumorigenesis.

Methods: Lentivirus infection, RT-PCR, Western blotting and tumorigenesis test *in vitro* and *in vivo* were performed.

Results: our results suggest that mutant MEG3 promotes the growth of human liver cancer stem cells *in vivo* and *in vitro*. Mechanistically, our results show that mutant MEG3 enhances acetylation modification of Histone H4 on K16. Then, mutant MEG3 enhances the expression of SETD2 dependent on H4K16Ac. Moreover, mutant MEG3 increases the DNA damage repair through SETD2. Ultimately, mutant MEG3 increases the telomerase activity dependent on DNA damage repair. Strikingly, TERT determines the cancerous function of mutant MEG3 in liver cancer stem cells. Therefore, we shed light on the fact that targeting mutant MEG3 could be a viable approach for cancer treatment.

Conclusions: these observations will play an important role in finding effective tumor treatment targets.

Background

A maternally expressed gene 3 (MEG3) acts as an antitumor component in different cancer cells, such as breast, liver, glioma, colorectal, cervical cancer cells. The biological function of MEG3 to repress tumor is through regulating the major tumor suppressor genes p53 and Rb (1). Mutant MEG3 has been shown to confer cancer susceptibility (2). MEG3 silencing induces DNA damage and inhibits EC proliferation (3) and MEG3 inhibits the progression of prostate cancer by modulating miR-9-5p/QKI-5 axis (4).

Furthermore, MEG3 regulates JAK/STAT pathway in chronic myeloid leukemia (5) and MEG3 targeting miR-424-5p via MAPK signaling pathway mediates neuronal apoptosis (6). Certain polymorphisms within MEG3 are implicated in cancer risk (rs7158663, rs4081134 and rs11160608) (7). Furthermore, MEG3 promotes Nlrp3-mediated microglial inflammation by targeting miR-7a-5p and regulates apoptosis of adipose-derived stem cells (8–10). Interestingly, MEG3 inhibits the inflammatory response of ankylosing spondylitis by targeting miR-146a (11) and suppresses the progression of ankylosing spondylitis (12). However, MEG3 promotes melanoma growth, metastasis and formation through modulating miR-21/E-cadherin axis (13) and modified epithelial-mesenchymal transition of ovarian cancer cells (14).

Telomere shortening is related to the onset of age-related disease (15). Telomere homeostasis generally results in gross genomic instability (16). Telomere loop dynamics play a role in chromosome end protection (17). Multiple cancer pathways regulate telomere protection (18). Telomere integrity is essential for genome stability and it regulates cell proliferation and tissue renewal (19). Moreover, telomere damage induces internal loops that generate telomeric circles (20).

In this study, we clearly demonstrate that mutant MEG3 promotes the growth of human liver cancer stem cells *in vivo* and *in vitro*. Mutant MEG3 enhances acetylation modification of Histone H4K16 and then enhances the expression of SETD2. Therefore, mutant MEG3 increases the DNA damage repair through SETD2 and increases the telomerase activity. These observations will play an important role in finding effective tumor treatment targets.

Materials And Methods

Tetracycline (DOX) inducing lentiviral rLV-tet on-mutant MEG3 The expression plasmid pLVX-tet on-Tight-EF1a-ZsGreen and pLVX-mutant MEG3-ZsGreen-Puro were digested with SpeI and NotI, respectively, and the large fragment of plasmid pLVX-tet on-Tight-EF1a-ZsGreen and the small fragment pLVX-mutant MEG3-ZsGreen-Puro were recovered by 1% agarose gel electrophoresis respectively. The two plasmid pLVX-tet on-Tight-EF1a-ZsGreen (SpeI + NotI) and pUC57-mutant MEG3(SpeI + NotI) were carried out the ligation reaction at 22 ° C for 3 hours and then the ligation products were transformed into JM109 competent bacterial overnight. Monoclonal colonies were picked for sequencing verification. The recombinant plasmid pLVX-tet on-mutant MEG3-Tight-EF1a-ZsGreen containing the gene of interest was transfected into 293T cells to generate a high titer lentivirus containing the gene of interest (rLV-tet on CircHULC).

CD133+/CD44 + Huh7 cells sorting CD133/CD44 MicroBead Kits were purchased from Miltenyi technic(Boston,USA) and MACS® Technology operation according to and the operation according to the manufacturer.

RT-PCR cDNA was prepared by using oligonucleotide (dT), random primers, and a SuperScript First-Strand Synthesis System (Invitrogen). PCR analysis was performed according to the manufacturer. β -actin was used as an internal control.

Western Blotting Proteins were separated on a 10% sodium dodecyl sulfate-polyacrylamide gel electrophoresis (SDS-PAGE) and transferred onto a nitrocellulose membranes (Invitrogen). And then blocked in 10% dry milk-TBST (20mM Tris-HCl [PH 7.6], 127mM NaCl, 0.1% Tween 20) for 1 h at 37°C. Following three washes in Tris-HCl pH 7.5 with 0.1% Tween 20, the blots were incubated with antibody(appropriate dilution) overnight at 4°C. Signals were visualized by enhanced chemiluminescence plus kit(GE Healthcare).

RNA Immunoprecipitation(RIP) Ribonucleoprotein particle-enriched lysates were incubated with protein G/A-plus agarose beads (Santa Cruz) together with antibody or normal rabbit IgG for 4 hours at 4°C. Beads were subsequently washed. RNAs were isolated and then RT-PCR.

Super-RNA-EMSA Cells were washed and scraped in ice-cold PBS to prepare nuclei for electrophoretic gel mobility shift assay with the use of the gel shift assay system (Promega) modified according to the manufacturer's instructions.

CHIP assay Cells were cross-linked with 1% (v/v) formaldehyde (Sigma) for 10 min at room temperature and stopped with 125 mM glycine for 5 min. Crossed-linked cells were washed with phosphate-buffered saline, resuspended in lysis buffer, and sonicated for 8–10 min in a SONICS VibraCell to generate DNA fragments. Chromatin extracts were diluted 5-fold with dilution buffer, pre-cleared with Protein-A/G-Sepharose beads, and immunoprecipitated with specific antibody on Protein-A/G-Sepharose beads. After washing, elution and de-cross-linking, the ChIP DNA was detected by PCR.

DNA damage repair assay DNA damage marker rH2AX (S139) detection, in situ DNA damage analysis and Quantitative analysis of DNA Damgae via 8-OHdG were performed according to the manufacturer's instructions, respectively.

Cell colony-formation efficiency assay cells were plated in six wells and incubated in a humidified atmosphere of 5% CO₂ incubator at 37°C for 14 days. For visualization, colonies were stained with 0.5% Crystal Violet (sigma) in 50% methanol and 10% glacial acetic acid. Colonies were counted using a dissecting microscope by MacBiophotonics Image J.

Tumorigenesis testin vivo Four-weeks male athymic Balb/c mice were maintained in the Tongji university animal facilities approved by the China Association for accreditation of laboratory animal care. athymic Balb/c mice per group were injected at the armpit area subcutaneously with cells. The mice were observed over 4 weeks for tumor formation. The mice were then sacrificed and the tumors recovered. The wet weight of each tumor was determined for each mouse. A portion of each tumor was fixed in 4% paraformaldehyde and embedded in paraffin for histological examination.

Results

Mutant MEG3 promotes malignant growth of human liver cancer stem cells

To investigate the ability of mutant MEG3 to promote the malignant growth of human liver cancer stem cells, we first used CD133/CD44/CD24/EpCAM beads to isolate human liver cancer stem cells (hLCSCs) from Huh7 cells (**Figure S1A**). In hLCSCs, CD133, CD44, CD24 and EpCAM were positively expressed (**Figure S1B&C**). The mutant MEG3 was cloned into the pLVX-Tet-on-Tight-EF1a-ZsGreen-circ plasmid, and the tetracycline (DOX)-regulated lentivirus rLVX-Tet-on-mutant MEG3 was prepared (rLV-tet on- mutant MEG3). The hLCSCs were infected with rLV-tet on- mutant MEG3. In the rLVX-Tet-on- mutant MEG3-hLCSCs treated with DOX (0µg/ml), DOX (0.5µg/ml), DOX (1µg/ml), DOX (1.5µg/ml), DOX (2µg/ml), mutant MEG3 was significantly increased with increasing DOX concentration (Fig. 1A&B). Cell growth ability (24hours: P = 0.0396, 0.0015, 0.014, 0.117; 48hours: P = 0.0013, 0.0056, 0.0086, 0.0377) (Fig. 1C), colony forming ability (38.3 ± 2.86% vs 49.4 ± 5.45%, p = 0.01; 49.4 ± 5.45% vs 61.75 ± 2.93%, p = 0.0068 < 0.01; 61.75 ± 2.93% vs 72.18 ± 2.8%, p = 0.0285 < 0.05; 72.18 ± 2.8% vs 88.19 ± 6.78, p = 0.0308 < 0.05) (Fig. 1D). The average weight of xenograft tumor (0.13 ± 0.024 gram vs 0.24 ± 0.038 gram, p = 0.0000005 < 0.01; 0.24 ± 0.038 gram vs 0.55 ± 0.076 gram, p = 0.0000017 < 0.01; 0.55 ± 0.076 gram vs 0.669 ± 0.07gram, p =

0.00022 < 0.01; 0.669 ± 0.07 gram vs 0.906 ± 0.04 gram, p = 0.00000048 < 0.01) (Fig. 1E&F), the appearance time of xenograft tumors in nude mice (10.8 ± 1.93 days vs 8.5 ± 2.55 days, p = 0.0245 < 0.05; 8.5 ± 2.55 days vs 7 ± 0.81 days, p = 0.043 < 0.05; 7 ± 0.81 days vs 6.1 ± 0.875 days, p = 0.0338 < 0.05; 6.1 ± 0.875 days vs 5.3 ± 1.06 days, p = 0.026 < 0.05) (Fig. 1G) were significantly increased with the increase of DOX concentration. Collectively, the results suggest that mutant MEG3 promotes the growth of human liver cancer stem cells *in vivo and in vitro*.

Mutant MEG3 enhances the modification of H4K16Ac

To investigate whether mutant MEG3 affects the acetylation modification of HistoneH4K16 in liver cancer stem cells, the stable human liver cancer stem cell lines (hLCSCs) infected with rLV-tet on-mutant MEG3 were subjected to different concentrations of DOX (0µg/ml, 0.5µg/ml, 1µg/ml, 1.5µg/ml, 2µg/ml) treatment. In stable hLCSCs in DOX (0µg/ml) treatment group, DOX (0.5µg/ml) treatment group, DOX (1µg/ml) treatment group, DOX (1.5µg/ml) treatment group, DOX (2µg/ml) treatment group, the expression of Sirt1 was significantly decreased with increasing DOX concentration (Fig. 2A). The interaction between Sirt1 and HistoneH4 was significantly decreased with increasing DOX concentration (Fig. 2B). H4K16Ac was significantly increased with increasing DOX concentration (Fig. 2C). Although H4K16Ac was significantly increased in DOX (2µg/ml) treatment group compared to DOX (0µg/ml) treatment group, it was significantly altered in DOX (2µg/ml) treatment + rLV-Sirt1 group compared to DOX (0µg/ml) treatment group (Fig. 2D). Collectively, these results suggest that mutant MEG3 enhances acetylation modification of HistoneH4K16 in human liver cancer stem cells.

Mutant MEG3 enhances the expression of SETD2 dependent on H4K16Ac

Given that mutant MEG3 enhances H4K16Ac, we consider to confirm whether mutant MEG3 enhances the expression of SETD2 through H4K16Ac. In DOX (0µg/ml) treatment group, DOX (0.5µg/ml) treatment group, DOX (1µg/ml) Treatment group, DOX (1.5µg/ml) treatment group, DOX (2µg/ml) treatment group, the loading of H4K16Ac onto SETD2 promoter were significantly increased with the increase of DOX concentration (Fig. 3A). The binding ability of H4K16Ac to SETD2 promoter probe was significantly increased with the increase of DOX concentration (Fig. 3B). The ability of RNA polymerase II and H4K16Ac to enter the SETD2 promoter-enhancer loop was significantly increased with the increase of DOX concentration (Fig. 3C). The SETD2 promoter transcription activity was significantly increased with the increase of DOX concentration (6648.22 ± 1064.21 vs 14004.22 ± 1577.31, p = 0.0083 < 0.01; 14004.22 ± 1577.31 vs 30941.04 ± 5106.58, p = 0.01199 < 0.05; 14004.22 ± 1577.31 vs 85439.01 ± 5949.46, p = 0.00412 < 0.01; 14004.22 ± 1577.31 vs 259763.9 ± 26836.33, p = 0.0041978 < 0.01) (Fig. 3D). The ability of SETD2 transcription and translation expression was significantly increased with the increase of DOX concentration (Fig. 3E). Collectively, these results suggest that mutant MEG3 enhances the expression of SETD2.

Mutant MEG3 increases the DNA damage repair through SETD2

Given that mutant MEG3 enhances the expression of SETD2, we consider whether mutant MEG3 increases the DNA damage repair through SETD2. In DOX (0µg/ml) treatment group, DOX (0.5µg/ml) treatment group, DOX (1µg/ml) treatment group, DOX (1.5µg/ml) treatment group, DOX (2µg/ml) treatment group, the interaction between SETD2 and HistoneH3 was significantly increased with the increase of DOX concentration (Fig. 4A). The H3K36me3 was significantly increased with the increase of DOX concentration(Fig. 4B). Although H3K36me3 was significantly increased in DOX (2µg/ml) treatment group, it was not significantly altered in DOX (2µg/ml) treatment + pGFP-V-RS-SETD2 group compared to DOX (2µg/ml) treatment group(Fig. 4C). The interaction among H3K36me3, Rad51, PARP1,ATR,ATM, hMSH6 and HistoneH3 was significantly increased with the increase of DOX concentration (Fig. 4D). The rH2AX(S139) was significantly decreased with the increase of DOX concentration(Fig. 4E). Although rH2AX(S139) was significantly decreased in DOX (2µg/ml) treatment group, it was not significantly altered in DOX (2µg/ml) treatment + pGFP-V-RS-SETD2 group compared to DOX (2µg/ml) treatment group(Fig. 4F). The DNA damage repair ability was significantly increased with the increase of DOX concentration (3.52 ± 0.28 vs 2.17 ± 0.07 , $p = 0.01$; 2.17 ± 0.07 vs 1.82 ± 0.066 , $p = 0.005 < 0.01$; 1.82 ± 0.066 vs 1.14 ± 0.075 , $p = 0.0005 < 0.01$; 1.14 ± 0.075 vs 0.77 ± 0.04 , $p = 0.007 < 0.01$) (Fig. 4G).

Collectively, these results suggest that mutant MEG3 increases the DNA damage repair through SETD2.

Mutant MEG3 increases the telomeras activity dependent on DNA damage repair

Given that mutant MEG3 increases the DNA damage repair through SETD2, we consider whether mutant MEG3 increases the telomeras activity dependent on DNA damage repair. In DOX (0µg/ml) treatment group, DOX (0.5µg/ml) treatment group, DOX (1µg/ml) Treatment group, DOX (1.5µg/ml) treatment group, DOX (2µg/ml) treatment group, the TERT expression was significantly increased with the increase of DOX concentration(Fig. 5A) .Although TERT was significantly increased in DOX (2µg/ml) treatment group, it was not significantly altered in DOX (2µg/ml) treatment + Rucaparib group compared to DOX (2µg/ml) treatment group(Fig. 5B). The interaction between TERT and TERC was significantly increased with the increase of DOX concentration (Fig. 5C). The telomease activity was significantly increased with the increase of DOX concentration (0.0153 ± 0.003 vs 0.033 ± 0.002 , $p = 0.0028 < 0.01$; 0.033 ± 0.002 vs 0.048 ± 0.001 , $p = 0.01$; 0.048 ± 0.0025 vs 0.0623 ± 0.003 , $p = 0.0038 < 0.01$; 0.0623 ± 0.003 vs 0.083 ± 0.017 , $p = 0.0039 < 0.01$) (Fig. 5D). The telomease lengths was significantly increased with the increase of DOX concentration (0.78 ± 0.059 vs 1.253 ± 0.04 , $p = 0.0049 < 0.01$; 1.253 ± 0.04 vs 1.85 ± 0.07 , $p = 0.0014 < 0.01$; 1.85 ± 0.07 vs 2.20 ± 0.097 , $p = 0.0013 < 0.01$; 2.20 ± 0.097 vs 3.1 ± 0.165 , $p = 0.00529 < 0.01$) (Fig. 5D). Collectively, these results suggest that mutant MEG3 increases the telomerase activity dependente on DNA damage repair.

TERT determines the cancerous function of mutant MEG3

Given that mutant MEG3 increases the telomerase activity dependent on DNA damage repair, we consider whether TERT determines the cancerous function of mutant MEG3. The expression of mutant MEG3 was

significantly increased in the DOX (2µg/ml) group, DOX (2µg/ml) + pGFP-V-RS-TERT group compared with the DOX (0µg/ml) group. The expression of TERT was significantly increased in the DOX (2µg/ml) group and decreased in DOX (2µg/ml) + pGFP-V-RS-TERT group compared with the DOX (0µg/ml) group (**Figure 6A**). Although the cell proliferation ability was significantly increased in the DOX (2µg/ml) group compared with the DOX (0µg/ml) group (24hours: $p=0.00063<0.01$; 48 hours: $p=0.0003<0.01$), it was not significantly altered in DOX (2µg/ml) + pGFP-V-RS-TERT group compared with the DOX (0µg/ml) group (24hours: $p=0.2266>0.05$; 48 hours: $p=0.1915>0.05$) (**Figure6B**). Although the colony formation ability was significantly increased in the DOX (2µg/ml) group compared with the DOX (0µg/ml) group ($45.04\pm6.91\%$ vs $80.23\pm9.54\%$, $p=0.0026<0.01$), it was not significantly altered in DOX (2µg/ml) + pGFP-V-RS-TERT group compared with the DOX (0µg/ml) group ($45.04\pm6.91\%$ vs $51.56\pm4.202\%$, $p=0.134>0.05$) (**Figure6C**). Although the weight of xenograft tumor in nude mice was significantly increased in the DOX (2µg/ml) group compared with the DOX (0µg/ml) group (0.53 ± 0.089 gram vs 1.06 ± 0.16 gram, $p=0.00053<0.01$), it was not significantly altered in DOX (2µg/ml) + pGFP-V-RS-TERT group compared with the DOX (0µg/ml) group (0.53 ± 0.089 gram vs 0.56 ± 0.106 gram, $p=0.279>0.05$) (**Figure6D&E**). Although the appearance time of xenograft tumor was significantly decreased in the DOX (2µg/ml) group compared with the DOX (0µg/ml) group (9.5 ± 1.05 days vs 6.33 ± 0.82 days, $p=0.002<0.01$), it was not significantly altered in DOX (2µg/ml) + pGFP-V-RS-TERT group compared with the DOX (0µg/ml) group (9.5 ± 1.05 days vs 9.0 ± 1.67 days, $p=0.328>0.05$) (**Figure6F**). Although the PCNA positive rate was significantly increased in the DOX (2µg/ml) group compared with the DOX (0µg/ml) group ($46.86\pm4.31\%$ vs $79.58\pm7.28\%$, $p=0.0000172<0.01$), it was not significantly altered in DOX (2µg/ml) + pGFP-V-RS-TERT group compared with the DOX (0µg/ml) group ($46.86\pm4.31\%$ vs $51.47\pm6.67\%$, $p=0.1807>0.05$) (**Figure6G**). Collectively, these observations suggest that TERT determines the cancerous function of mutant MEG3.

Discussion

At the present, we clearly demonstrate that mutant MEG3 promotes the growth of human liver cancer stem cells *in vivo and in vitro*. Mechanistically, our results shows that mutant MEG3 enhances acetylation modification of HistoneH4K16. Then, mutant MEG3 enhances the expression of SETD2 dependent on H4K16Ac. Furthermore, mutant MEG3 increases the DNA damage repair through SETD2. Ultimately, mutant MEG3 increases the telomeras activity dependent on DNA damage repair. In particular, TERT determines the cancerous function of mutant MEG3 in liver cancer stem cells (Fig. 6H). These observations will play an important role in finding effective tumor treatment targets.

First, our results indicate that mutant MEG3 promotes the growth of human liver cancer stem cells *in vivo and in vitro*. LncRNA-MEG3 inhibits cell proliferation and invasion by modulating Bmi1/RNF2 in cholangiocarcinoma(21). Also, MEG3 inhibits HMEC-1 cells growth, migration and tube formation via sponging miR-147(22).

Secondly, our results suggest that mutant MEG3 enhances acetylation modification of HistoneH4K16 dependent on Sirt1 in human liver cancer stem cells. Sirtuin-1 (SIRT1) is a class-III histone deacetylase

(HDAC), an NAD⁺-dependent enzyme deeply involved in gene regulation, genome stability maintenance, apoptosis, autophagy, senescence, proliferation, aging, and tumorigenesis(23). Sirt1 also appears to be important for the turnover of defective mitochondria by mitophagy(24).SIRT1 regulates macrophage self-renewal(25) and regulates lipid metabolism, oxidative stress and inflammation in the liver (26).Furthermore,SIRT1 has recently garnered tremendous attention because of its various regulatory effects in several pathological conditions(27).In additional, ATGL promotes autophagy/lipophagy via SIRT1 to control hepatic lipid droplet catabolism(28).H4K16Ac acts as epigenetic signatures of diffuse intrinsic pontine glioma(29).Selective binding of the PHD6 finger of MLL4 to histone H4K16Ac links MLL4 and MOF(30).JMJD6 modulates DNA damage response through downregulating H4K16Ac independently of its enzymatic activity(31).Acetylation of hMOF modulates H4K16Ac to regulate DNA repair genes (32, 33).

Moreover, our results demonstrate mutant MEG3 enhances the expression of SETD2 dependent on H4K16Ac. SETD2 restricts prostate cancer metastasis by integrating EZH2 and AMPK signaling pathways(34). SETD2-dependent histone H3K36 trimethylation is required for homologous recombination repair and genome stability(35).The H3 lysine 36 histone methyltransferase SETD2 is mutated across a range of human cancers (36). Loss of SETD2 promotes K-ras-induced acinar-to-ductal metaplasia and epithelia-mesenchymal transition during pancreatic carcinogenesis(37). Also, SETD2 acts as a regulator of N6-methyladenosine RNA methylation and modifiers in cancer(38).SETD2 mutations confer chemoresistance in acute myeloid leukemia partly through altered cell cycle checkpoints(39). Furthermore, SETD2 regulates cancer development(40).Dual chromatin and cytoskeletal was remodeled by SETD2(41).Interestingly, SETD2 mutation suppress autophagy via regulation of ATG12(42).

Notably, our results suggest that mutant MEG3 increases the DNA damage repair through H3K36me3 dependent on SETD2. There are diverse clues showing H3K36me3 participates in DNA damage response by directly recruiting DNA repair machinery to set the chromatin at a "ready" status (43). Histone H3 trimethylation at lysine 36 guides m⁶A RNA modification co-transcriptionally(44, 45). Chromosome 3P loss of heterozygosity reduces expression of H3K36me3 in sacral conventional chordoma (46). Furthermore, gene body DNA methylation conspires with H3K36me3 to preclude aberrant transcription(47).DNA damage is related to the balance between survival and death in cancer biology (48).As exemplified in diverse cancers,disruption or deregulation of DNA repair pathways results in genome instability(49).Moreover, the DNA mismatch repair triggers cell cycle arrest in some cases(50).The DNA damage respons makes it safe to play with knives(51). Cell fate regulation is associated with upon DNA damage(52, 53).

Intriguingly, we clearly identity that mutant MEG3 increases the telomeras activity dependent on DNA damage repair. Furthermore, our results indicate that TERT determines the cancerous function of mutant MEG3. Telomerase, an RNA-dependent DNA polymerase with telomerase reverse transcriptase (TERT), regulates cancer formation(54, 55).A particular attention is given to the putative connections between TERT transcriptional reactivation and signalling pathways frequently altered in cancer, such as c-MYC,

NF- κ B and β -Catenin(56). TERT promoter mutations are associated with poor prognosis and cell immortalization in meningioma(57).DNA methylation of the TERT promoter is associated with human cancer(58).TERT and TERC mutations suppress telomerase activity(59).TERT C228T mutation is associated with intravesical recurrence for patients with non-muscle invasive bladder cancer(60).TERC is an RNA component of telomerase and TERC promotes cellular inflammatory response independent of telomerase(61). HuR regulates telomerase activity through TERC methylation(62). Mitochondrion-processed TERC regulates senescence without affecting telomerase activities(63).C-MYC drives overexpression of telomerase RNA (hTR/TERC) (64). In particular,the TERC haploinsufficiency affects on the inheritance of telomere length(65) and is involved in the process of genetic instability leading to tumorigenesis (66).

In conclusions, the present study will focus on studying the effective mechanism of mutant MEG3 in carcinogenesis. These studies will play an important role in finding effective tumor treatment targets.

Abbreviations

maternally expressed gene 3 (MEG3)

Tetracycline (DOX)

RNA Immunoprecipitation(RIP)

Sirtuin-1 (SIRT1)

telomerase reverse transcriptase (TERT)

Declarations

Ethics approval and consent to participate

All methods were carried out in "accordance" with the approved guidelines. All experimental protocols "were approved by" a Tongji university institutional committee. Informed consent was obtained from all subjects. The study was reviewed and approved by the China national institutional animal care and use committee.

Consent for publication

'Not applicable'

Availability of data and material

'Not applicable'

Competing interests

"The authors declare that they have no competing interests"

Funding

This study was supported by grants from National Natural Science Foundation of China (NCSF No.8127229181773158 [NCSF No.82073130]) and by grants from Science and Technology Commission of Shanghai Municipality Shanghai Science and Technology Plan Basic Research Field Project [19JC1415200] and by grants from Science and Technology Commission of Shanghai Municipality Shanghai Science and Technology Plan Basic Research Field Project [20JC1411400].

Authors' contributions

Dongdong Lu conceived the study and participated in the study design, performance, coordination and manuscript writing. Shuting Song, Sijie Xie, Rushi Qin, Yanan Lu, Liyan Wang, Yingjie Chen, Xiaoxue Jiang, performed the research. All authors have read and approved the final manuscripts.

Acknowledgements

This study was supported by grants from National Natural Science Foundation of China (NCSF No.8127229181773158 [NCSF No.82073130]) and by grants from Science and Technology Commission of Shanghai Municipality Shanghai Science and Technology Plan Basic Research Field Project [20JC1411400] and by grants from Science and Technology Commission of Shanghai Municipality Shanghai Science and Technology Plan Basic Research Field Project [19JC1415200].

References

1. Al-Rugeebah A, Alanazi M, Parine NR. MEG3: an Oncogenic Long Non-coding RNA in Different Cancers. *Pathol Oncol Res.* 2019;25(3):859–74.
2. Ali MA, Shaker OG, Alazrak M, AbdelHafez MN, Khalefa AA, Hemeda NF, Abdelmuktader A, Ahmed FA. Association analyses of a genetic variant in long non-coding RNA MEG3 with breast cancer susceptibility and serum MEG3 expression level in the Egyptian population. *Cancer Biomark.* 2020;28(1):49–63.
3. Shihabudeen Haider Ali MS, Cheng X, Moran M, Haemmig S, Naldrett MJ, Alvarez S, Feinberg MW, Sun X. LncRNA Meg3 protects endothelial function by regulating the DNA damage response. *Nucleic Acids Res.* 2019;47(3):1505–22.
4. Wu M, Huang Y, Chen T, Wang W, Yang S, Ye Z, Xi X. LncRNA MEG3 inhibits the progression of prostate cancer by modulating miR-9-5p/QKI-5 axis. *J Cell Mol Med.* 2019;23(1):29–38.
5. Li ZY, Yang L, Liu XJ, Wang XZ, Pan YX, Luo JM. The Long Noncoding RNA MEG3 and its Target miR-147 Regulate JAK/STAT Pathway in Advanced Chronic Myeloid Leukemia. *EBioMedicine.* 2018;34:61–75.

6. Xiang Y, Zhang Y, Xia Y, Zhao H, Liu A, Chen Y. LncRNA MEG3 targeting miR-424-5p via MAPK signaling pathway mediates neuronal apoptosis in ischemic stroke. *Aging (Albany NY)*. 2020;12(4):3156–3174.
7. Ghafouri-Fard S, Taheri M. Maternally expressed gene 3 (MEG3): A tumor suppressor long non coding RNA. *Biomed Pharmacother*. 2019 Oct;118:109129.
8. Meng J, Ding T, Chen Y, Long T, Xu Q, Lian W, Liu W. LncRNA-Meg3 promotes Nlrp3-mediated microglial inflammation by targeting miR-7a-5p. *Int Immunopharmacol*. 2021;90:107141.
9. Shi Y. MEG3 regulates apoptosis of adipose-derived stem cells. *Mol Med Rep*. 2020;21(6):2435–42.
10. Wang A, Hu N, Zhang Y, Chen Y, Su C, Lv Y, Shen Y. MEG3 promotes proliferation and inhibits apoptosis in osteoarthritis chondrocytes by miR-361-5p/FOXO1 axis. *BMC Med Genomics*. 2019;12(1):201.
11. Li Y, Zhang S, Zhang C, Wang M. LncRNA MEG3 inhibits the inflammatory response of ankylosing spondylitis by targeting miR-146a. *Mol Cell Biochem*. 2020;466(1–2):17–24.
12. Ma J, Zhang X, Zhang H, Chen H. IncRNA MEG3 Suppresses the Progression of Ankylosis Spondylitis by Regulating the Let-7i/SOST Axis. *Front Mol Biosci*. 2020 Jul 24;7:173.
13. Wu L, Zhu L, Li Y, Zheng Z, Lin X, Yang C. LncRNA MEG3 promotes melanoma growth, metastasis and formation through modulating miR-21/E-cadherin axis. *Cancer Cell Int*. 2020;20:12.
14. Wang L, Yu M, Zhao S. IncRNA MEG3 modified epithelial-mesenchymal transition of ovarian cancer cells by sponging miR-219a-5p and regulating. *EGFR J Cell Biochem*. 2019;120(10):17709–22.
15. Turner KJ, Vasu V, Griffin DK. Telomere Biology and Human Phenotype. *Cells*. 2019;8(1):73
16. Giardini MA, Segatto M, da Silva MS, Nunes VS, Cano MI. Telomere and telomerase biology. *Prog Mol Biol Transl Sci*. 2014;125:1–40.
17. Van Ly D, Low RRJ, Frölich S, Bartolec TK, Kafer GR, Pickett HA, Gaus K, Cesare AJ. Telomere Loop Dynamics in Chromosome End Protection. *Mol Cell*. 2018;71(4):510–25.
18. Bejarano L, Bosso G, Louzame J, Serrano R, Gómez-Casero E, Martínez-Torrecuadrada J, Martínez S, Blanco-Aparicio C, Pastor J, Blasco MA. Multiple cancer pathways regulate telomere protection. *EMBO Mol Med*. 2019;11(7):e10292.
19. Ahmed W, Lingner J. Impact of oxidative stress on telomere biology. *Differentiation*. 2018;99:21–7.
20. Mazzucco G, Huda A, Galli M, Piccini D, Giannattasio M, Pessina F, Doksani Y. Telomere damage induces internal loops that generate telomeric circles. *Nat Commun*. 2020;11(1):5297.
21. Li J, Jiang X, Li C, Liu Y, Kang P, Zhong X, Cui Y. LncRNA-MEG3 inhibits cell proliferation and invasion by modulating Bmi1/RNF2 in cholangiocarcinoma. *J Cell Physiol*. 2019;234(12):22947–59.
22. Xu D, Liu T, He L, Han D, Ma Y, Du J. LncRNA MEG3 inhibits HMEC-1 cells growth, migration and tube formation via sponging miR-147. *Biol Chem*. 2020;401(5):601–15.
23. Alves-Fernandes DK, Jasiulionis MG. The Role of SIRT1 on DNA Damage Response and Epigenetic Alterations in Cancer. *Int J Mol Sci*. 2019;20(13):3153.
24. Tang BL. Sirt1 and the Mitochondria. *Mol Cells*. 2016;39(2):87–95.

25. Imperatore F, Maurizio J, Vargas Aguilar S, Busch CJ, Favret J, Kowenz-Leutz E, Cathou W, Gentek R, Perrin P, Leutz A, Berruyer C, Sieweke MH. SIRT1 regulates macrophage self-renewal. *EMBO J*. 2017;36(16):2353–72.
26. Ding RB, Bao J, Deng CX. Emerging roles of SIRT1 in fatty liver diseases. *Int J Biol Sci*. 2017 Jul 6;13(7):852–867.
27. Zhao B, Li X, Zhou L, Wang Y, Shang P. SIRT1: a potential tumour biomarker and therapeutic target. *J Drug Target*. 2019;27(10):1046–52.
28. Sathyanarayan A, Mashek MT, Mashek DG. ATGL Promotes Autophagy/Lipophagy via SIRT1 to Control Hepatic Lipid Droplet Catabolism. *Cell Rep*. 2017;19(1):1–9.
29. An S, Camarillo JM, Huang TY, Li D, Morris JA, Zoltek MA, Qi J, Behbahani M, Kambhampati M, Kelleher NL, Nazarian J, Thomas PM, Saratsis AM. Histone tail analysis reveals H3K36me2 and H4K16ac as epigenetic signatures of diffuse intrinsic pontine glioma. *J Exp. Clin Cancer Res*. 2020;39(1):261.
30. Zhang Y, Jang Y, Lee JE, Ahn J, Xu L, Holden MR, Cornett EM, Krajewski K, Klein BJ, Wang SP, Dou Y, Roeder RG, Strahl BD, Rothbart SB, Shi X, Ge K, Kutateladze TG. Selective binding of the PHD6 finger of MLL4 to histone H4K16ac links MLL4 and. *MOF Nat Commun*. 2019;10(1):2314.
31. Huo D, Chen H, Cheng Y, Song X, Zhang K, Li MJ, Xuan C. JMJD6 modulates DNA damage response through downregulating H4K16ac independently of its enzymatic activity. *Cell Death Differ*. 2020;27(3):1052–66.
32. Zhong J, Ji L, Chen H, Li X, Zhang J, Wang X, Wu W, Xu Y, Huang F, Cai W, Sun ZS. Acetylation of hMOF Modulates H4K16Ac to Regulate DNA Repair Genes in Response to Oxidative Stress. *Int J Biol Sci*. 2017;13(7):923–34.
33. Sheikh BN, Guhathakurta S, Akhtar A. The non-specific lethal (NSL) complex at the crossroads of transcriptional control and cellular homeostasis. *EMBO Rep*. 2019 Jul;20(7):e47630.
34. Yuan H, Han Y, Wang X, Li N, Liu Q, Yin Y, Wang H, Pan L, Li L, Song K, Qiu T, Pan Q, Chen Q, Zhang G, Zang Y, Tan M, Zhang J, Li Q, Wang X, Jiang J, Qin J. SETD2 Restricts Prostate Cancer Metastasis by Integrating EZH2 and AMPK Signaling Pathways. *Cancer Cell*. 2020;38(3):350–65.
35. Pfister SX, Ahrabi S, Zalmas LP, Sarkar S, Aymard F, Bachrati CZ, Helleday T, Legube G, La Thangue NB, Porter AC, Humphrey TC. SETD2-dependent histone H3K36 trimethylation is required for homologous recombination repair and genome stability. *Cell Rep*. 2014;7(6):2006–18.
36. Fahey CC, Davis IJ. SETting the Stage for Cancer Development: SETD2 and the Consequences of Lost Methylation. *Cold Spring Harb Perspect Med*. 2017;7(5):a026468.
37. Niu N, Lu P, Yang Y, He R, Zhang L, Shi J, Wu J, Yang M, Zhang ZG, Wang LW, Gao WQ, Habtezion A, Xiao GG, Sun Y, Li L, Xue J. Loss of SETD2 promotes K-ras-induced acinar-to-ductal metaplasia and epithelia-mesenchymal transition during pancreatic carcinogenesis. *Gut*. 2020;69(4):715–726.
38. Kumari S, Muthusamy S. SETD2 as a regulator of N6-methyladenosine RNA methylation and modifiers in cancer. *Eur. J Cancer Prev*. 2020;29(6):556–64.

39. Dong Y, Zhao X, Feng X, Zhou Y, Yan X, Zhang Y, Bu J, Zhan D, Hayashi Y, Zhang Y, Xu Z, Huang R, Wang J, Zhao T, Xiao Z, Ju Z, Andreassen PR, Wang QF, Chen W, Huang G. SETD2 mutations confer chemoresistance in acute myeloid leukemia partly through altered cell cycle checkpoints. *Leukemia*. 2019;33(11):2585–2598.
40. McDaniel SL, Strahl BD. Shaping the cellular landscape with Set2/SETD2 methylation. *Cell Mol Life Sci*. 2017;74(18):3317–34.
41. Park IY, Powell RT, Tripathi DN, Dere R, Ho TH, Blasius TL, Chiang YC, Davis IJ, Fahey CC, Hacker KE, Verhey KJ, Bedford MT, Jonasch E, Rathmell WK, Walker CL. Dual Chromatin Cytoskeletal Remodeling by SETD2. *Cell*. 2016;166(4):950–62.
42. González-Rodríguez P, Engskog-Vlachos P, Zhang H, Murgoci AN, Zerdas I, Joseph B. SETD2 mutation in renal clear cell carcinoma suppress autophagy via regulation of ATG12. *Cell Death Dis*. 2020;11(1):69.
43. Sun Z, Zhang Y, Jia J, Fang Y, Tang Y, Wu H, Fang D. H3K36me3, message from chromatin to DNA damage repair. *Cell Biosci*. 2020;10:9.
44. Huang H, Weng H, Zhou K, Wu T, Zhao BS, Sun M, Chen Z, Deng X, Xiao G, Auer F, Klemm L, Wu H, Zuo Z, Qin X, Dong Y, Zhou Y, Qin H, Tao S, Du J, Liu J, Lu Z, Yin H, Mesquita A, Yuan CL, Hu YC, Sun W, Su R, Dong L, Shen C, Li C, Qing Y, Jiang X, Wu X, Sun M, Guan JL, Qu L, Wei M, Müschen M, Huang G, He C, Yang J, Chen. *J Nature*. 2019;567(7748):414–9.
45. Weinberg DN, Papillon-Cavanagh S, Chen H, Yue Y, Chen X, Rajagopalan KN, Horth C, McGuire JT, Xu X, Nikbakht H, Lemiesz AE, Marchione DM, Marunde MR, Meiners MJ, Cheek MA, Keogh MC, Bareke E, Djedid A, Harutyunyan AS, Jabado N, Garcia BA, Li H, Allis CD, Majewski J, Lu C. The histone mark H3K36me2 recruits DNMT3A and shapes the intergenic DNA methylation landscape. *Nature*. 2019;573(7773):281–6.
46. Zhu GG, Ramirez D, Chen W, Lu C, Wang L, Frosina D, Jungbluth A, Ntiamoah P, Nafa K, Boland PJ, Hameed MR. Chromosome 3p loss of heterozygosity and reduced expression of H3K36me3 correlate with longer relapse-free survival in sacral conventional chordoma. *Hum Pathol*. 2020;104:73–83.
47. Teissandier A, Bourc'his D. Gene body DNA methylation conspires with H3K36me3 to preclude aberrant transcription. *EMBO J*. 2017;36(11):1471–3.
48. Roos WP, Thomas AD, Kaina B. DNA damage and the balance between survival and death in cancer biology. *Nat Rev Cancer*. 2016;16(1):20–33.
49. Chatterjee N, Walker GC. Mechanisms of DNA damage, repair, and mutagenesis. *Environ Mol Mutagen*. 2017;58(5):235–63.
50. Li Z, Pearlman AH, Hsieh P. DNA mismatch repair and the DNA damage response. *DNA Repair*. 2016;38:94–101.
51. Ciccia A, Elledge SJ. The DNA damage response: making it safe to play with knives. *Mol Cell*. 2010;40(2):179–204.
52. Bantele SCS, Pfander B. Quantitative mechanisms of DNA damage sensing and signaling. *Curr Genet*. 2020;66(1):59–62.

53. Liebl MC, Hofmann TG. Cell Fate Regulation upon DNA Damage: p53 Serine 46 Kinases Pave the Cell Death Road. *Bioessays*. 2019;41(12):e1900127.
54. Yuan X, Xu D. Telomerase Reverse Transcriptase (TERT) in Action: Cross-Talking with Epigenetics. *Int J Mol Sci*. 2019;20(13):3338. TERT regulates cancer formation.
55. Dratwa M, Wysoczańska B, Łacina P, Kubik T, Bogunia-Kubik K. TERT-Regulation and Roles in Cancer Formation. *Front Immunol*. 2020;11:589929.
56. Pestana A, Vinagre J, Sobrinho-Simões M, Soares P. TERT biology and function in cancer: beyond immortalisation. *J Mol Endocrinol*. 2017;58(2):R129–46.
57. Spiegl-Kreinecker S, Lötsch D, Neumayer K, Kastler L, Gojo J, Pirker C, Pichler J, Weis S, Kumar R, Webersinke G, Gruber A, Berger W. TERT promoter mutations are associated with poor prognosis and cell immortalization in meningioma. *Neuro Oncol*. 2018;20(12):1584–93.
58. Lee DD, Komosa M, Nunes NM, Tabori U. DNA methylation of the TERT promoter and its impact on human cancer. *Curr Opin Genet Dev*. 2020;60:17–24.
59. Terada K, Miyake K, Yamaguchi H, Miyake N, Yamanaka K, Kojima S, Ito E, Inokuchi K, Okada T. TERT and TERC mutations detected in cryptic dyskeratosis congenita suppress telomerase activity. *Int J Lab Hematol*. 2020;42(3):316–21.
60. Hayashi Y, Fujita K, Nojima S, Tomiyama E, Matsushita M, Koh Y, Nakano K, Wang C, Ishizuya Y, Kato T, Hatano K, Kawashima A, Ujike T, Uemura M, Imamura R, Morii E, Nonomura N. recurrence for patients with non-muscle invasive bladder cancer. *Mol Oncol*. 2020;14(10):2375–83.
61. Liu H, Yang Y, Ge Y, Liu J, Zhao Y. TERC promotes cellular inflammatory response independent of telomerase. *Nucleic Acids Res*. 2019;47(15):8084–95.
62. Tang H, Wang H, Cheng X, Fan X, Yang F, Zhang M, Chen Y, Tian Y, Liu C, Shao D, Jiang B, Dou Y, Cong Y, Xing J, Zhang X, Yi X, Songyang Z, Ma W, Zhao Y, Wang X, Ma J, Gorospe M, Ju Z, Wang W. HuR regulates telomerase activity through TERC methylation. *Nat Commun*. 2018;9(1):2213.
63. Zheng Q, Liu P, Gao G, Yuan J, Wang P, Huang J, Xie L, Lu X, Di F, Tong T, Chen J, Lu Z, Guan J, Wang G. Mitochondrion-processed TERC regulates senescence without affecting telomerase activities. *Protein Cell*. 2019;10(9):631–48.
64. Baena-Del Valle JA, Zheng Q, Esopi DM, Rubenstein M, Hubbard GK, Moncaliano MC, Hruszkewycz A, Vaghasia A, Yegnasubramanian S, Wheelan SJ, Meeker AK, Heaphy CM, Graham MK, De Marzo AM. MYC drives overexpression of telomerase RNA (hTR/TERC) in prostate cancer. *J Pathol*. 2018;244(1):11–24.
65. Goldman F, Bouarich R, Kulkarni S, Freeman S, Du HY, Harrington L, Mason PJ, Londoño-Vallejo A, Bessler M. The effect of TERC haploinsufficiency on the inheritance of telomere length. *Proc Natl Acad Sci U S A*. 2005;102(47):17119–24.
66. Goldberg-Bittman L, Kitay-Cohen Y, Fejgin MD, Hadary R, Quitt M, Amiel A. TERC telomerase subunit gene copy number in different disease stages of non-hodgkin lymphoma and in hepatitis C. *Cancer Invest*. 2010;28(2):181–5.

Figures

Figure 1

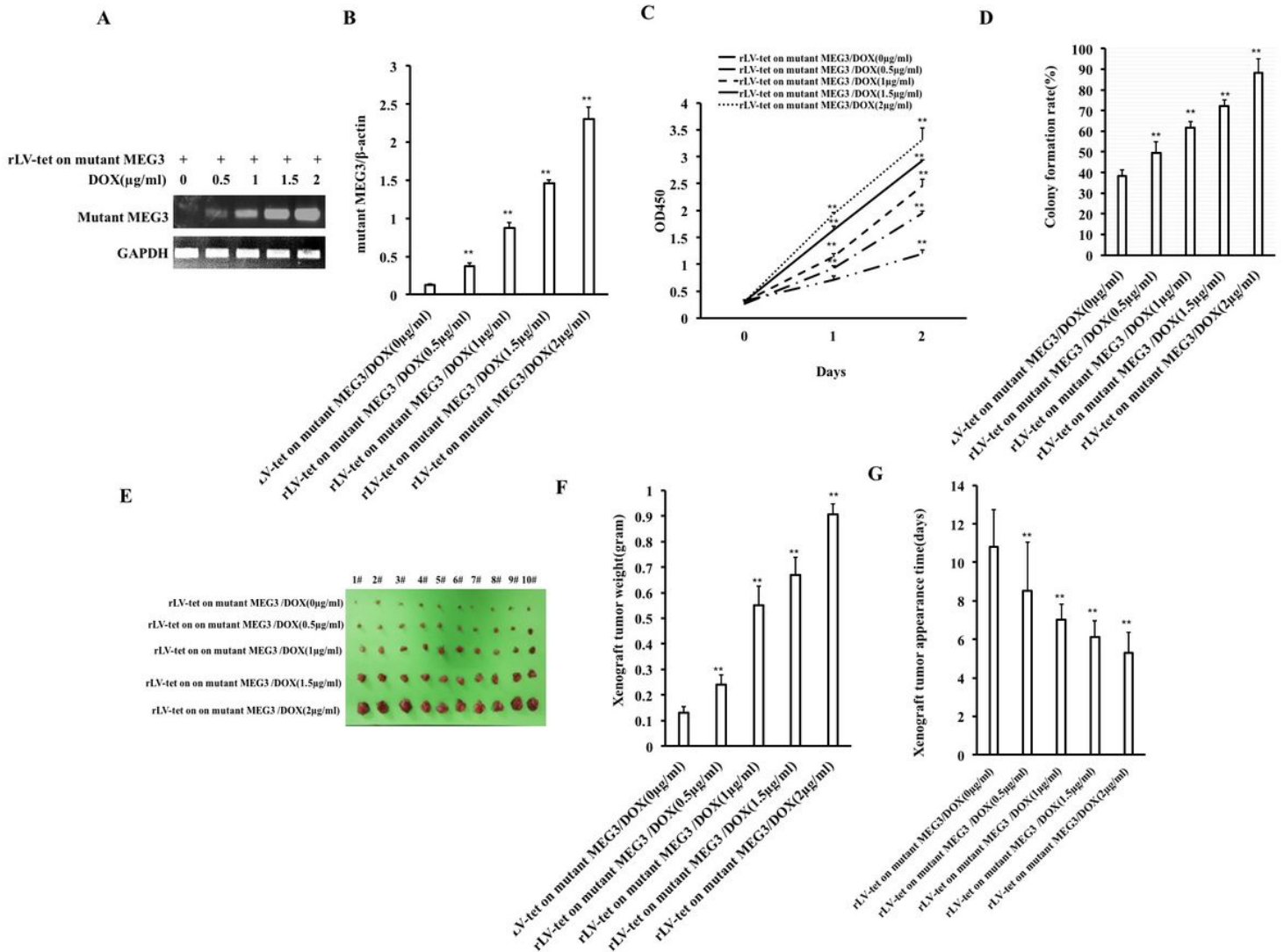
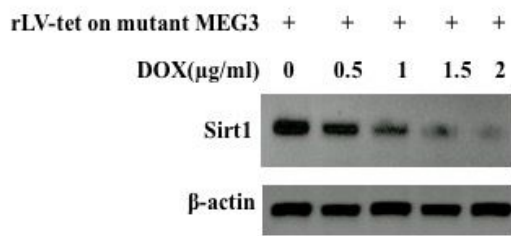


Figure 1

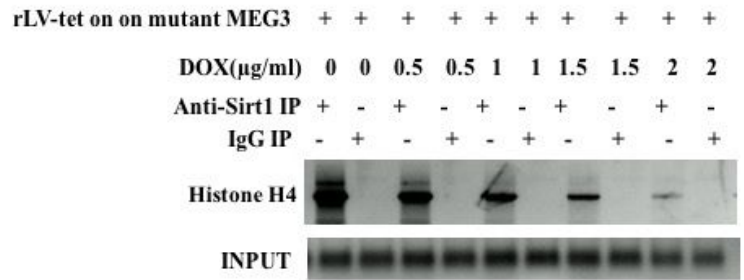
mutant MEG3 promotes the growth of human liver cancer stem cells in vitro and in vivo. A&B. RT-PCR was used to detect of mutant MEG3 in the cells at different concentrations of DOX (0 μ g / ml, 0.5 μ g / ml, 1 μ g / ml, 1.5 μ g / ml, 2 μ g / ml) (A. semi-quantitative; B. quantitative). β -actin serves as an internal reference. C. Growth curve assay using CCK8. D. The crystal violet staining method was used to determine the plate colony forming ability. The analysis of colony formation rate. E. Photos of transplanted tumors (xenograft). F. Comparison of the size (g) of transplanted tumors. G. Comparison of the appearance time (days) of transplanted tumors. **, P < 0.01 or *, P < 0.05 means statistical difference is significant.

Figure 2

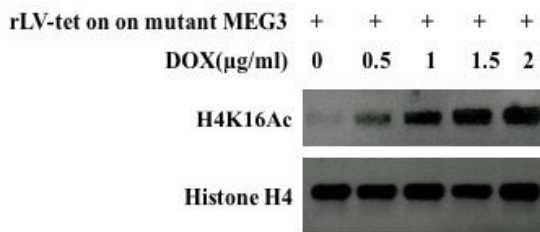
A



B



C



D

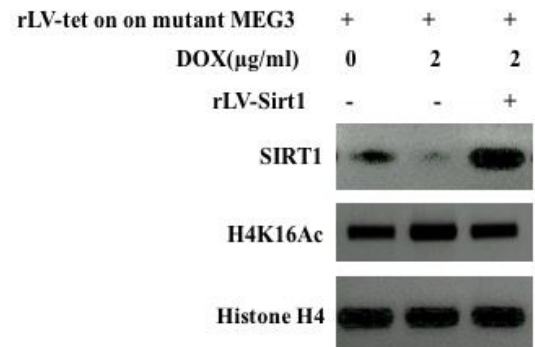
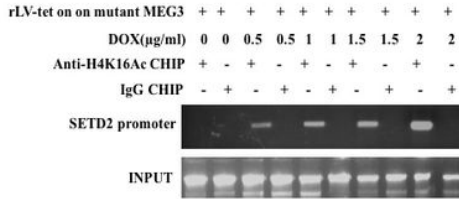


Figure 2

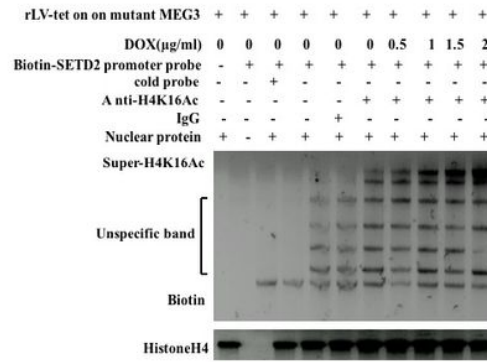
Mutant MEG3 enhances the modification of H4K16Ac. A. Immunoblot analysis with anti-Sirt1. β-actin serves as an internal reference. B. Co-immunoprecipitation analysis with anti-Sirt1 and anti-HistoneH4. C. Immunoblot analysis with anti-H4K16Ac. HistoneH4 serves as an internal reference. D. Immunoblot analysis with anti-H4K16Ac and anti-Sirt1. HistoneH4 serves as an internal reference.

Figure3

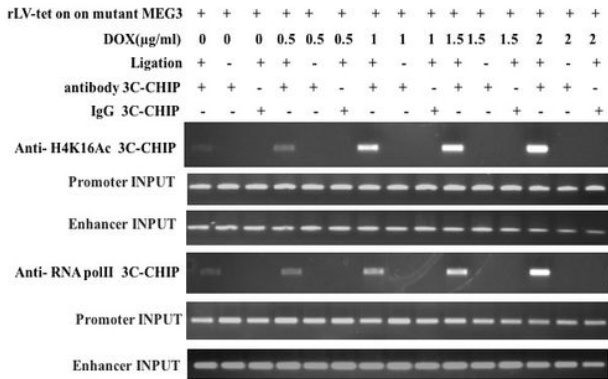
A



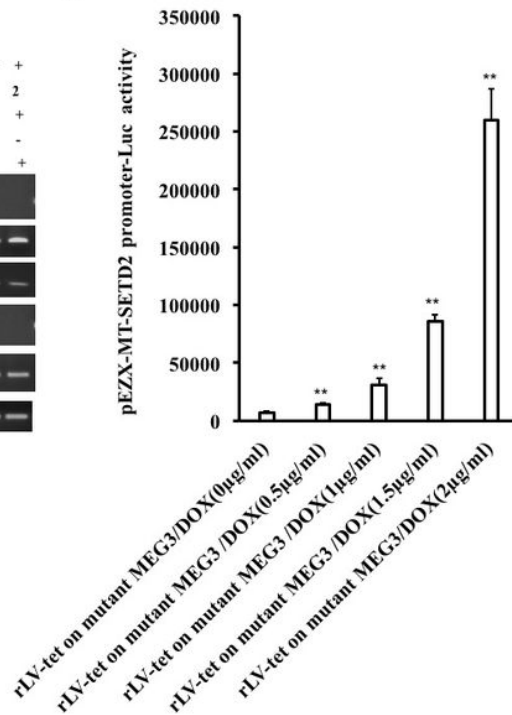
B



C



D



E

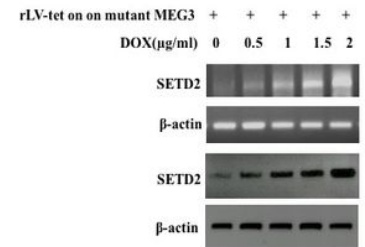


Figure 3

Mutant MEG3 enhances the expression of SETD2 dependent on H4K16Ac. A. Chromatin immunoprecipitation analysis with anti-H4K16Ac in rLV-Tet-on-circ mutant MEG3-hLCSCs. B. Super-DNA gel migration assay (EMSA) analysis with anti-H4K16Ac and Biotin-SETD2 probe. C. Chromosome conformation capture-chromatin immunoprecipitation analysis with anti-H4K16Ac and SETD2 promoter-enhancer probe. D. The assay of pEZX-MT-SETD2 promoter-Luc luciferase activity. E. RT-PCR analysis of SETD2 transcriptional ability and Western blotting analysis with anti-SETD2. β -actin serves as an internal reference gene.

Figure 4

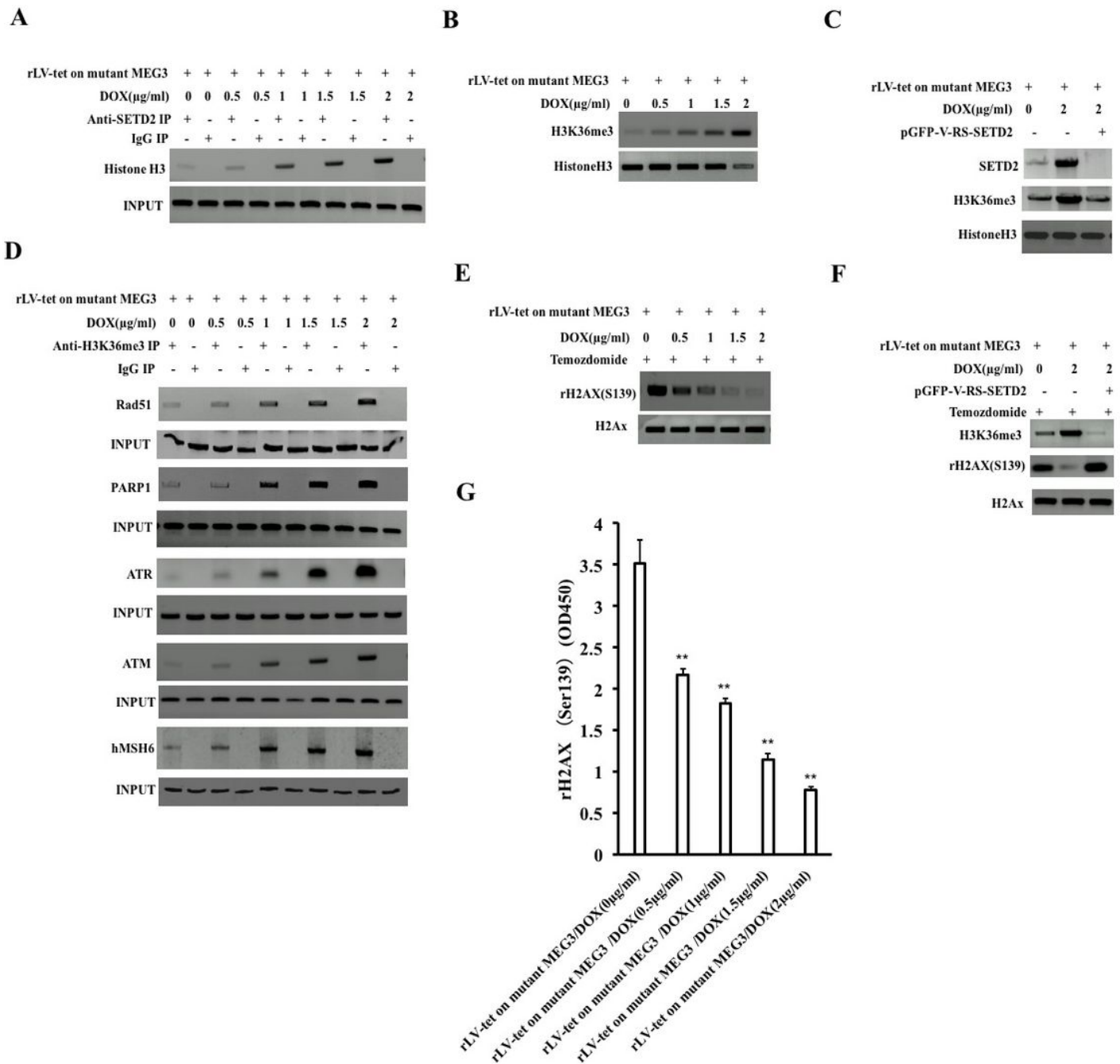


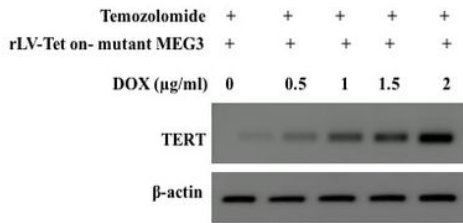
Figure 4

Mutant MEG3 increases the DNA damage repair through SETD2. A. Co-immunoprecipitation analysis with anti-SETD2 and anti-HistoneH3. B&C. Immunoblot analysis with anti-H4K36me3 and anti-SETD2. HistoneH3 serves as an internal reference. D. Co-immunoprecipitation analysis with anti- H3K36me3 , anti- Rad51, anti-PARP1, anti-ATR, anti-ATM, anti-hMSH6. a. E. RT-PCR analysis of SETD2 transcriptional ability and Western blotting analysis with anti-SETD2. β -actin serves as an internal reference gene. E&F. Immunoblot analysis with anti- rH2AX(S139). H2AX serves as an internal reference.G. The assay of DNA

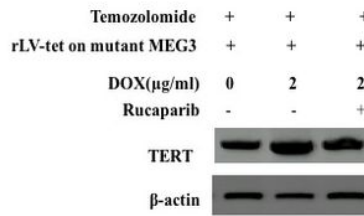
damage repair ability. The values of each group were expressed as mean \pm SEM (n =3), **, P < 0.01, and *, P < 0.05, respectively.

Figure 5

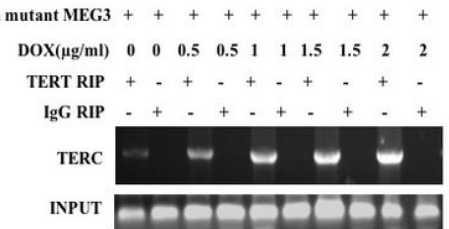
A



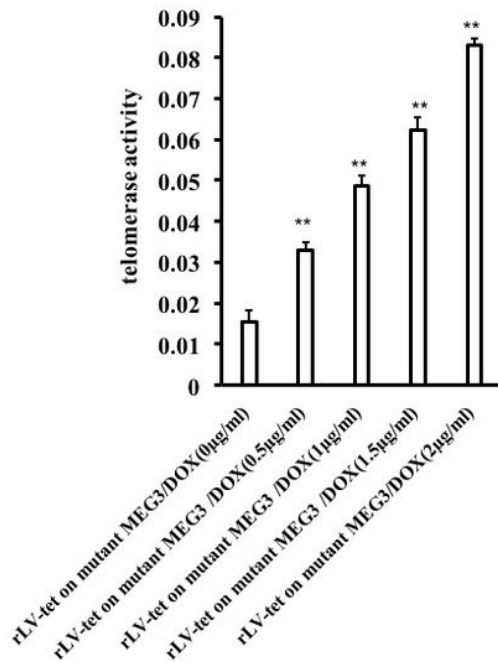
B



C



D



E



Figure 5

mutant MEG3 increases the telomerase activity dependent on DNA damage repair. A&B. Immunoblot analysis with anti-TERT. β -actin serves as an internal reference. C. RNA immunoprecipitation analysis with anti-TERC. RT-PCR for TERC. D. The assay of telomerase activity. The values of each group were expressed as mean \pm SEM (n =3), **, P < 0.01, and *, P < 0.05, respectively. E. The assay of telomere length. The values of each group were expressed as mean \pm SEM (n =3), **, P < 0.01, and *, P < 0.05, respectively.

Figure6

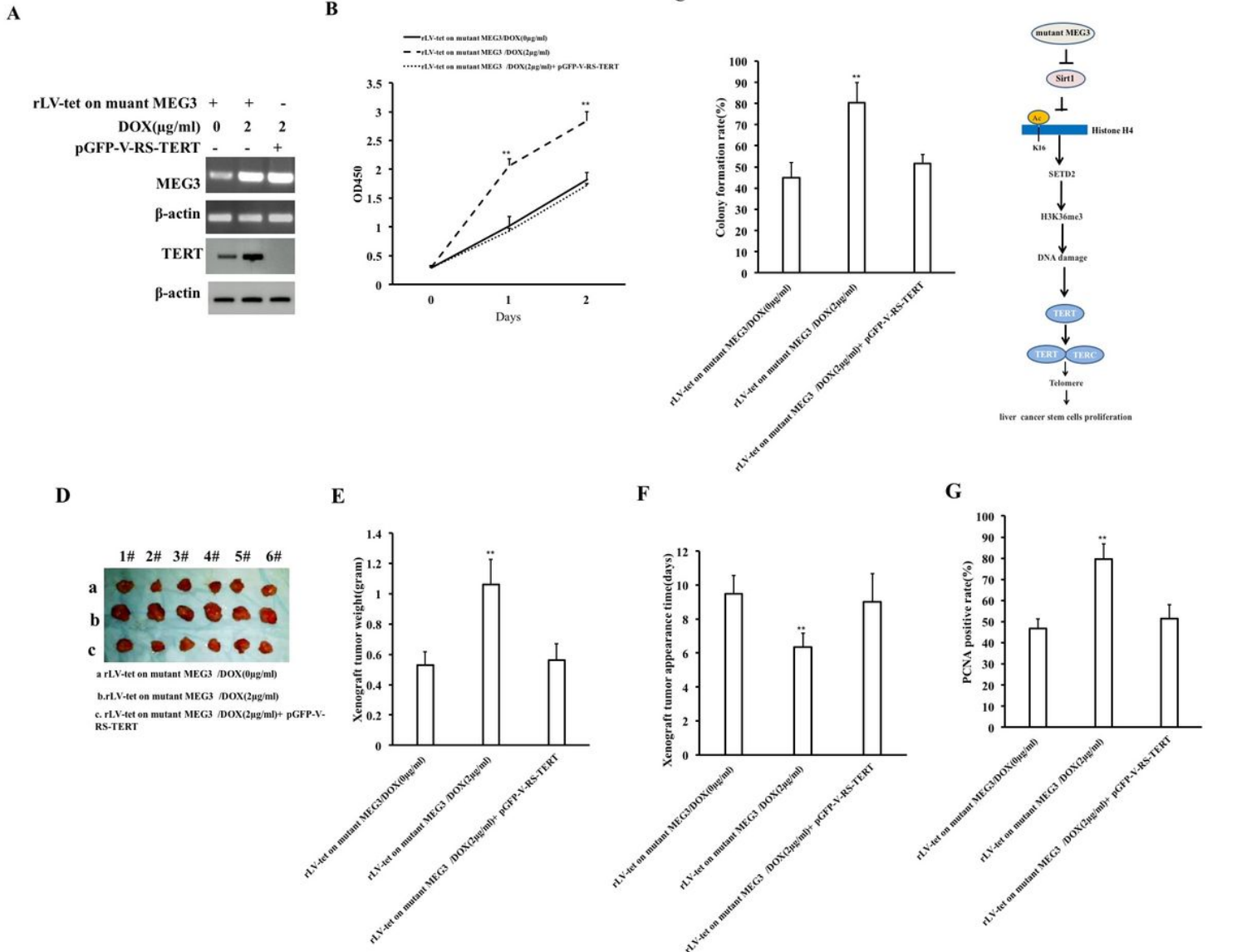


Figure 6

TERT determines the cancerous function of mutant MEG3. A. RT-PCR analysis of mutant MEG3 and immunoblotting analysis with anti-TERT. B. Determination of cell proliferation using CCK8. Each experiment was repeated three times. Each group of values is expressed as mean \pm standard deviation (mean \pm SEM, n = 3), **, P < 0.01, *, P < 0.05. C. Determination of cell colony forming ability. D. Photograph of transplanted tumors dissected. E. Comparison of the size (grams) of transplanted tumors in nude mice. Each experiment was repeated three times. Each group of values is expressed as mean \pm standard deviation (mean \pm SEM, n = 6), **, P < 0.01, *, P < 0.05. F. Comparison of the time (days) for the appearance of transplanted tumors in nude mice. G. anti-PCNA immunohistochemical staining. Each group of values is expressed as mean \pm standard deviation (mean \pm SD, n = 6), **, P < 0.01, *, P < 0.05. H. Schematic

diagram of the mechanism by which mutant MEG3 enhances the activity of telomerase by enhancing DNA damage repair in human liver cancer stem cells.

Supplementary Files

This is a list of supplementary files associated with this preprint. Click to download.

- [Supplementaldata.docx](#)